

Coupled-Channel Schrödinger-Equation Model for High-Energy Peripheral Collisions*

JOHN G. WILLS, DAVID ELLIS,† AND D. B. LICHTENBERG
Physics Department, Indiana University, Bloomington, Indiana
 (Received 15 October 1965)

We have considered a model for high-energy pion-nucleon scattering in which there are 3 (or 4) open channels— πN , ρN , πN^* (and ρN^*)—and in which the scattering is determined by coupled Schrödinger equations with Yukawa potentials corresponding to exchange of a single π or ρ meson. All particles are considered spinless for simplicity, and relativistic kinematics are used. The calculations are done numerically on a CDC-3600 computer, in the partial-wave representation, for all values of the orbital angular momentum that contribute significantly to the cross sections. The results are compared with those of 4 other approximations: (1) simple Born approximation, (2) Born approximation modified by absorption parameters taken from elastic scattering, (3) the unitary S matrix obtained by identifying the Born approximation with the K matrix, (4) Born approximation modified by absorption parameters determined in a self-consistent way from the optical theorem. We find that none of the approximate methods agree in detail with the coupled-channel Schrödinger-equation results, but that methods (2), (3) and (4) agree qualitatively with the coupled-channel method for the reaction $\pi N \rightarrow \rho N$ near the forward direction.

I. INTRODUCTION

WHEN two strongly interacting particles collide at high energy, a great many different things can happen: The number of possible final states increases rapidly with the energy. Because there are many strongly coupled channels, a calculation of the scattering into any one channel is not likely to be successful if it ignores the effects of all the others. The most obvious effect is that of absorption: The competition of the other processes reduces the incident wave, and so decreases the amplitude in question.

Fortunately, some simplifying features are also present in many high-energy reactions. One such feature is the tendency for multiparticle final states to contain resonant combinations of particles. This leads to the approximation of considering only two-body final states, in which either or both of the particles may be unstable. A second simplifying feature is that the angular distributions of these two-body final states are often sharply peaked in the forward direction. This leads to the use of the peripheral model, in which only one-particle exchange is considered, so as to account for the long-range part of the interaction.

In addition to providing qualitative agreement with the observed forward peaking of the production cross sections, the peripheral model, calculated in lowest order Born approximation, also gives, in many cases, an approximately correct prediction for the decay angular distributions of the unstable particles. However, these calculations do not agree quantitatively with experiment. In a number of cases the total cross sections calculated by the Born approximation have come out far too large. In almost all cases the observed angular distribution is much more peaked in the forward direction than the angular distribution calculated from the single-particle exchange diagrams. While there are many explanations which might be given for these

quantitative failures of the model, probably the most obvious criticism is that the existence of all the other competing processes has been ignored. Evidence that such a procedure can not be right is provided by the fact that if one makes a partial-wave expansion of the Born-approximation amplitude one finds that the partial-wave amplitudes often exceed the unitarity limit in the lower partial waves. When several such strong processes are going on at once, they cannot be treated independently.

The idea of combining the simple peripheral model with the fact of many competing reaction channels has led to much of the recent work in analysis of high-energy inelastic scattering—particularly in the production of meson and baryon resonances. One method of taking into account the effects of competing channels on any given reaction is to use the distorted-wave Born approximation with a complex potential in the elastic channel. Summerfield¹ has applied this method to production of hyperon-antihyperon pairs in nucleon-antinucleon annihilation. An even simpler way to reduce the Born-approximation results so as to account for the competition of other open channels, is to multiply the Born amplitude by initial-state and final-state absorption parameters, which are deduced from elastic-scattering experiments. An approximation of this kind was first used in high-energy physics by Sopkovich.² Subsequently, similar or identical approximations have been used by Durand and Chiu,³ Ross and Shaw,⁴ Gottfried and Jackson,⁵ and many others. Gottfried and Jackson have pushed this method further than any one else and have obtained quite good agreement with many experiments, especially in those cases involving exchange of pseudoscalar mesons. Since the absorption parameters are always less than one, the

¹ G. C. Summerfield, *Nuovo Cimento* **23**, 867 (1962).

² N. J. Sopkovich, *Nuovo Cimento* **26**, 186 (1962).

³ L. Durand and Y. Chiu, *Phys. Rev. Letters* **12**, 399 (1964).

⁴ M. Ross and G. Shaw, *Phys. Rev. Letters* **12**, 627 (1964).

⁵ K. Gottfried and J. D. Jackson, *Nuovo Cimento* **34**, 735 (1964).

* Work supported in part by the National Science Foundation.
 † Present address: Physics Department, University of Toledo, Toledo, Ohio.

method of Sopkovich is a way of lessening the extent of violation of unitarity by the Born approximation. This technique will be described in a little more detail later.

Of course the Sopkovich method, although currently one of the most popular methods of partially unitarizing the Born-approximation result, is not the only method for doing this. There is also, for example, the so-called K -matrix approximation, used by Arnold⁶ and by Dietz and Pilkuhn,⁷ among others, in which the Born-approximation amplitude is identified with the K matrix. Using this approximation, one can construct S -matrix elements which satisfy unitarity exactly. Another method devised by Williams and one of us (DBL)⁸ makes use of the Sopkovich formula but does not take the absorption parameters from experiment. Rather, the method allows one to calculate them, using the unitarity condition of the S matrix. This is a method which makes the magnitudes of the S -matrix elements unitary but does not make the S matrix completely unitary. Other methods make use of dispersion relations, using for example the so-called N/D method.⁹ All these approximation methods are designed to improve the unitary properties of the lowest order Born approximation. But making the Born approximation unitary is certainly not a unique prescription. Thus, although a nonunitary approximation must be wrong, a unitary one is not necessarily right.

Both the modified and the unmodified peripheral models give much better agreement with experiment in cases which seem to involve the exchange of a spinless meson, than in reactions where it is reasonable to assume that a meson of higher spin is exchanged. In particular, the one vector meson exchange diagram predicts the wrong energy dependence of the cross section. The calculated value of the cross section increases as the energy of the incident particle increases, whereas in the actual experiment the cross section decreases rather rapidly as the energy increases. This difficulty is connected with the well-known difficulties of field theories of particles of spin 1 or greater, when calculated in perturbation theory. We shall confine our considerations to spinless particles, and shall have nothing to say about this particular problem.

A different way of modifying the peripheral model has been to postulate that form factors must be introduced into the one-particle exchange diagrams. A number of people have had some success in this approach. In particular, Ferrari and Selleri¹⁰ have been able to obtain rather good agreement with a wide variety of data using a single phenomenological form factor which is a function of the square of the four-momentum transfer. However, the use of a form

factor is rather unsatisfactory because it is hard to give physical significance to parameters in the expression assumed for the form factor.

A number of theoretical papers have been written attempting to justify the validity of many of the approximations discussed, in particular those based on the method of Sopkovich.¹¹ These papers have shown that under certain conditions the approximations are indeed good ones. However, in general, it is easiest to show that the improvements on the Born approximation are good when the Born approximation elements themselves are small and also give rather good agreement with the predictions of an exact calculation. There are certain other conditions under which the approximation also can be justified. We shall not go into a technical discussion of these conditions. However, we think it is fair to say that the use of these approximations has not been fully justified under the conditions that are believed to hold in high-energy collisions. For this reason, we have devised a potential model which we can solve numerically to any desired accuracy and which incorporates many of the features believed to hold in the actual high-energy problem. We then compare the prediction of some of the approximation methods to the predictions of our model when solved numerically. A comparison of various approximation methods with some exactly solvable models has been carried out by Kantor.¹² Kantor considered only scattering in $l=0$ states, whereas we consider all the partial waves necessary (more than 20) to produce the forward peak in high-energy scattering.

It is the main purpose of this paper to describe the model and its numerical solution, and to give a comparison of the approximation methods with the predictions of this model. The model is as follows: We consider only states in which two particles go in and two particles come out. Each state of two particles is considered a channel. All particles are taken to be spinless. We assume that the interaction between particles is of the form of a Yukawa potential, which, for an n -channel problem, is an n -by- n potential matrix. This potential matrix can lead to scattering from a given initial channel to any final channel which conserves energy. We assume that the exact solution to our model is the S matrix that is obtained by putting our n -by- n potential matrix into a Schrödinger equation, and solving the resulting n coupled equations. Although these equations are basically nonrelativistic, we use the relativistic connection between the momentum of any channel and its energy. We also use reduced energies rather than reduced masses in the equations. In other words, we use a nonrelativistic Schrödinger equation with relativistic kinematics. This coupled-channel Schrödinger equation is then

⁶ R. C. Arnold, Phys. Rev. **136**, B1388 (1964).

⁷ K. Dietz and H. Pilkuhn (to be published).

⁸ D. B. Lichtenberg and P. K. Williams, Phys. Rev. **139**, B179 (1965).

⁹ P. Coulter, A. Scotti, and G. Shaw, Phys. Rev. **36**, 1399 (1964).

¹⁰ E. Ferrari and F. Selleri, Nuovo Cimento Suppl. **24**, 453 (1962).

¹¹ L. Durand and Y. Chiu, Phys. Rev. **139**, B428 (1965); R. Omnes, *ibid.* **137**, B649 (1965); E. J. Squires, Nuovo Cimento **34**, 1328 (1964); J. Ball and W. Frazer, Phys. Rev. Letters **14**, 746 (1965).

¹² P. B. Kantor, Ann. Phys. (N. Y.) **33**, 196 (1965).

solved numerically and the S matrix elements and differential cross sections are obtained.

To make the model as realistic as possible, we use dimensionless coupling constants for the Yukawa potentials of the order of unity, corresponding to the strengths of potentials to be expected in strong interactions. For the ranges of the Yukawa potentials we take ranges equal to the Compton wavelengths of mesons. For the masses of incoming and outgoing particles, we use masses equal to the masses of the observed strongly interacting particles. All this can be done without needlessly complicating the coupled-channel equations. However, we take the particles to be spinless because the inclusion of spin adds additional channels and therefore complicates the equations. We wanted to take a model as realistic as possible without unduly increasing the time needed to solve the equations numerically.

In addition to the Born approximation result, we compute the approximate predictions of the model of Sopkovich, the K -matrix approximation method, and the method of Lichtenberg and Williams. We have not used any of the methods based on dispersion relations. We compare the results of the approximate methods with the coupled channel calculation to test the validity of the various approximations in our particular model. The numerical calculation of the coupled-channel Schrödinger equation can be thought of as a computer experiment.

We make no comparison of any of our calculations with experiment, as our model is not realistic enough to warrant such a comparison. Rather, our purpose is to test the rather widely used approximation methods against a model which can be calculated precisely.

In Sec. II we describe the model and discuss how it is solved exactly by numerical solution of a coupled-channel Schrödinger equation. We also describe the various approximation methods to be tested. In Sec. III, we describe certain interesting features of the S -matrix elements and differential cross sections, as calculated by the coupled-channel Schrödinger equation method. The reader who is interested only in a comparison of the exact predictions of the model with the approximation methods may skip Sec. III and go on to Sec. IV, where this comparison is made. Our conclusions are given in Sec. V.

II. DESCRIPTION OF THE CALCULATIONS

We shall now discuss the parametrization of the S matrix and formulas for scattering amplitudes and cross sections in an n -channel problem. The differential cross section for scattering from channel α to channel β is given by

$$(d\sigma/d\Omega)_{\alpha\rightarrow\beta} = |f_{\alpha\beta}(\theta)|^2, \quad (1)$$

where the scattering amplitude is related to the partial-wave S matrix $S_{\alpha\beta}^{(l)}$ as follows:

$$f_{\alpha\beta}(\theta) = \frac{1}{2ip_\alpha} \sum_{l=0}^{\infty} (2l+1)[S_{\alpha\beta}^{(l)} - \delta_{\alpha\beta}]P_l(\cos\theta). \quad (2)$$

Here $\delta_{\alpha\beta}$ is the Kronecker delta, p_α is the center-of-mass-system momentum in channel α , and θ is the center-of-mass-system scattering angle. A number of authors^{5,6} have used the so-called impact-parameter representation in which the scattering amplitude is written as an integral over impact parameters rather than as a sum over partial waves. This approximation is useful at high energy when large numbers of partial waves contribute, and in some cases makes for simpler calculations. However, we shall concern ourselves exclusively with the partial wave representation.

The S -matrix elements can be parametrized either in terms of their real and imaginary parts or, more commonly, in terms of absorption parameters $\eta_{\alpha\beta}^{(l)}$ and real phase shifts $\delta_{\alpha\beta}^{(l)}$:

$$S_{\alpha\beta}^{(l)} = \epsilon_{\alpha\beta}\eta_{\alpha\beta}^{(l)} \exp(2i\delta_{\alpha\beta}^{(l)}), \quad \begin{aligned} \epsilon_{\alpha\beta} &= 1 & \text{if } \alpha = \beta \\ &= i & \text{if } \alpha \neq \beta. \end{aligned} \quad (3)$$

For simplicity, we sometimes drop the superscript l , or write it as a subscript when the indices α and β are absent.

The set of coupled Schrödinger equations which we use is as follows:

$$-\frac{\nabla^2}{2\lambda_\beta}\Phi_{\alpha\beta}(r) + \sum_{\gamma=1}^n V_{\beta\gamma}(r)\Phi_{\alpha\gamma}(r) = E_\beta\Phi_{\alpha\beta}(r). \quad (4)$$

The wave function $\Phi_{\alpha\beta}(r)$ describes scattering from channel α to channel β . We use relativistic kinematics, so that instead of the reduced mass, there appears λ_α the reduced total energy in channel α : $\lambda_\alpha = E_{1\alpha}E_{2\alpha}/(E_{1\alpha} + E_{2\alpha})$, where $E_{1\alpha}$ and $E_{2\alpha}$ are the energies of the two particles in the center-of-mass system. Also $E_\alpha = p_\alpha^2/2\lambda_\alpha$ takes the place of the kinetic energy, where p_α is the momentum of either particle in the center of mass system, computed relativistically. The potential energy is assumed to be of the form

$$V_{\alpha\beta}(r) = -g_{\alpha\beta}r^{-1} \exp(-\mu_{\alpha\beta}r), \quad (5)$$

where the $g_{\alpha\beta}$ are strength parameters and the $\mu_{\alpha\beta}$ are range parameters ($\hbar = c = 1$). The scattering amplitude from channel α to channel β appears in the asymptotic behavior of the wave function for large r :

$$\Phi_{\alpha\beta}(r) \sim \delta_{\alpha\beta} e^{ip_\alpha \cdot r} + \left(\frac{v_\alpha}{v_\beta}\right)^{1/2} f_{\alpha\beta}(\theta) r^{-1} \exp(ip_\beta r), \quad (6)$$

where v_α is the relative velocity $v_\alpha = p_\alpha/\lambda_\alpha$.

A partial wave analysis gives the differential equations to be solved

$$\Phi_{\alpha\beta}(r) = \sum_l r^{-1} u_{\alpha\beta}^{(l)}(r) P_l(\cos\theta) \quad (7)$$

$$\begin{aligned} \frac{d^2}{dr^2} u_{\alpha\beta}^{(l)}(r) + \left[p_\beta^2 - \frac{l(l+1)}{r^2} \right] u_{\alpha\beta}^{(l)}(r) \\ - 2\lambda_\beta \sum_\gamma V_{\beta\gamma}(r) u_{\alpha\gamma}^{(l)}(r) = 0. \end{aligned} \quad (8)$$

We obtain the S -matrix elements from the following boundary conditions:

$$u_{\alpha\beta}^{(l)}(r) \sim \frac{2l+1}{2} r i^l \left(\frac{p_\beta/v_\alpha}{p_\alpha/v_\beta} \right)^{1/2} \times [S_{\alpha\beta}^{(l)} h_l^{(1)}(p_\beta r) + \delta_{\alpha\beta} h_l^{(2)}(p_\beta r)], \quad (9)$$

where $h_l^{(1)}$ and $h_l^{(2)}$ are spherical Hankel functions of the first and second kind, respectively. Equations (8) were solved by direct numerical integration on the Indiana University CDC 3600 computer, using a modification of the program which one of us (JGW) had previously written for calculations of low-energy α -particle scattering. This procedure gives us what we call the exact coupled-channel result.

We now describe the approximation methods. The Born-approximation scattering amplitude is calculated in the usual way. We denote this result by $f_B(\theta)$, suppressing the channel indices α and β . We can expand the Born approximation amplitudes in partial waves, obtaining

$$f_B(\theta) = (1/2p) \sum_l (2l+1) B_l P_l(\cos\theta). \quad (10)$$

The Born approximation for the S matrix is denoted by $S_l(B) = 1 + iB_l$, or in more detail,

$$S_{\alpha\beta}^{(l)}(B) = \delta_{\alpha\beta} + [2ig_{\alpha\beta}/(v_\alpha v_\beta)^{1/2}] Q_l(\xi_{\alpha\beta}), \quad (11)$$

where Q_l is the Legendre function of the second kind, and

$$\xi_{\alpha\beta} = (\mu_{\alpha\beta}^2 + p_\alpha^2 + p_\beta^2)/2p_\alpha p_\beta. \quad (12)$$

The approximation first used by Sopkovich² is a method to obtain only the nondiagonal elements of the S matrix. The prescription is that the nondiagonal S -matrix elements are given by the following formula:

$$S_{\alpha\beta}^{(l)}(\text{SF}) = i(S_{\alpha\alpha}^{(l)})^{1/2} B_{\alpha\beta}^{(l)} (S_{\beta\beta}^{(l)})^{1/2}, \quad \alpha \neq \beta, \quad (13)$$

where the SF attached to the symbol for the S matrix stands for Sopkovich's formula. In this formula the diagonal elements $S_{\alpha\alpha}^{(l)}$ and $S_{\beta\beta}^{(l)}$ are supposed to be given by experiment. In our model we have no actual experiment, but we do have our computer experiment. Therefore in (13) we use the $S_{\alpha\alpha}^{(l)}$ and $S_{\beta\beta}^{(l)}$ as determined from the results of the coupled channel calculation.

The K -matrix method^{6,7} starts from the Born approximation B_l but obtains a unitary S matrix from B_l by the following matrix equation:

$$S_l(K) = (1 + \frac{1}{2}iB_l)(1 - \frac{1}{2}iB_l)^{-1}. \quad (14)$$

Since in this formula the relation between S_l and B_l is the conventional relation between S_l and the K matrix, we call this the K -matrix approximation.

The method developed by Lichtenberg and Williams⁷ again starts with the formula given in Eq. (13), but the elastic S -matrix elements are not determined from

the computer experiment. Rather, they are given by the following formulas:

$$S_{\alpha\alpha}^{(l)}(\text{LW}) = \eta_{\alpha\alpha}^{(l)}, \quad (15)$$

$$S_{\alpha\beta}^{(l)}(\text{LW}) = i(\eta_{\alpha\alpha}^{(l)})^{1/2} B_{\alpha\beta}^{(l)} (\eta_{\beta\beta}^{(l)})^{1/2} \text{ for } \alpha \neq \beta, \quad (16)$$

where

$$\eta_{\alpha\alpha}^{(l)} = [1 + \sum_{\gamma=1}^n B_{\alpha\gamma}^{(l)2}]^{-1/2}, \quad \gamma \neq \alpha. \quad (17)$$

See Ref. 7 for a discussion of these formulas.

In deciding what energy, what potential, and how many channels to use, we try to consider a realistic problem and at the same time try to minimize the computing time. First of all, the computing time in doing a coupled-channel calculation goes approximately as the cube of the number of channels. Therefore it is to our advantage to try to keep the number of channels as small as possible. Unfortunately, at high energy the number of channels in a realistic calculation is rather large and increases with increasing energy. Therefore we did not go to too high an energy. Another factor working against going to too high energy is that the value of the relative momentum increases with increasing energy and the wave function oscillates with a higher frequency. This means that smaller integration steps are needed for a given accuracy. Also, the number of partial waves which must be calculated increases with energy. Again, high-energy increases the length of computing time needed. However, if we go to too low an energy, the peripheral model is likely not to be valid at all. We compromise at taking incident laboratory momenta p_π between 1.6 and 4.0 BeV/ c .

We considered three- and four-channel problems. For the four-channel problem the channels considered were

$$\begin{aligned} \pi + N &\rightarrow \pi + N, \\ &\rightarrow \rho + N, \\ &\rightarrow \pi + \Delta, \\ &\rightarrow \rho + \Delta, \end{aligned} \quad (18)$$

where Δ is the πN resonance at a mass of 1238 MeV. For the three-channel problem the $\rho\Delta$ channel was omitted. We found that there was not very much qualitative difference between doing a four- and a three-channel problem.

The choice of the strengths and ranges of the Yukawa potentials presented a few difficulties. In addition to ignoring spin in the problem, we did not include isospin. Therefore, even in those cases in which the actual coupling constants are known, we have no valid criteria for obtaining the signs of the Yukawa potentials. We tried different choices of signs of the potentials to see what effect this would have. In some of the physical reactions shown in Eq. (18), one-pion exchange processes are allowed, and in other cases they are forbidden by G parity conservation. We used for the ranges of the

potentials the pion Compton wavelength if a pion is allowed to be exchanged, and a ρ -meson Compton wavelength if pion exchange is forbidden by G -parity conservation. To be precise, the model to which we gave the most attention is the 3-channel problem where channels 1, 2, and 3 represent πN , ρN , and $\pi\Delta$ states, respectively. The range parameters of the potentials [see Eq. (5)] are then given by

$$\mu_{\alpha\beta} = \begin{pmatrix} m_\rho & m_\pi & m_\rho \\ m_\pi & m_\rho & m_\pi \\ m_\rho & m_\pi & m_\rho \end{pmatrix}.$$

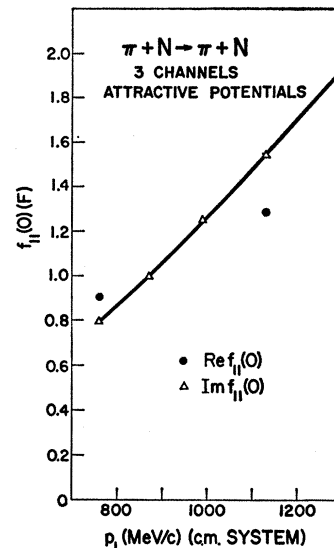
For most of our calculations, we assumed that all dimensionless coupling constants are equal to one. We considered various combinations as follows: All potentials negative (attractive), all potentials positive (repulsive), potentials with range equal to the pion Compton wavelength positive and potentials with ρ Compton wavelength negative, and vice versa. Of course the effect of a positive nondiagonal potential is not necessarily repulsive. For example, in a two-channel problem a nondiagonal potential has the same attractive effect independent of the sign of the potential. Also, since the range of the π -exchange potential is so much longer than that of the ρ -exchange potential, we also calculated the case in which *only* π exchange is considered; that is, the ρ -exchange coupling constants were set equal to zero.

III. GENERAL CHARACTER OF THE COUPLED-CHANNEL RESULTS

The peripheral nature of the scattering is clearly shown in the coupled channel cross sections. In all channels (elastic scattering and production of particles) the differential cross section shows a sharp peaking in the forward direction, dropping one or two orders of magnitude for momentum transfers $\gtrsim 3$ times the pion mass. At larger momentum transfers the behavior of the coupled channel cross section depends on details. The results depend on which channel we are considering and on whether the potentials are positive or negative. The coupled channel cross section may continue to fall as the angle increases, or there may be an abrupt change of slope and the angular distribution may become fairly flat at larger angles. However, the cross section at large angles is so small compared to the cross section in the forward angles that one would tend not to believe the model at these angles. In other words in actual high-energy reactions, effects such as exchange of heavier particles, effects of crossing symmetry, and many-body final states will make contributions to the cross section at angles which are large compared to the contributions from π exchange.

Although the model is unrealistic at the large angles, it is amusing to look at what the predictions are. If all potentials are attractive the elastic scattering cross section becomes relatively flat at large angles. However,

FIG. 1. Real and imaginary parts of the calculated pion-nucleon forward elastic scattering amplitude as a function of incident pion center-of-mass momentum p_1 . The solid line shows the imaginary part, and the circles show the real part. We give the real part at only two momenta, because a large amount of computing time is necessary to obtain sufficient precision. See text for further explanation.



if the one-pion-exchange potentials are attractive, whereas the ρ -exchange potentials are repulsive, there is a rapid drop in the elastic scattering cross section all the way to $\cos\theta = -1$. The cross section drops five orders of magnitude in this case between $\cos\theta = +1$ and -1 . It is only on a semilog plot, however, that the difference between the two cases can be seen. On a linear scale the cross sections at momentum transfers $\gtrsim 3$ pion masses are negligible, compared to the cross sections in the forward direction, in both cases.

A noteworthy feature of the coupled channel results is that the real part of the elastic scattering amplitude is important. Even if there is no ρ exchange, so that all elastic scattering results from the indirect effect of pion exchange, there is a large real part of the elastic scattering amplitude. In our problem, the real part often turns out to be greater than the imaginary part, even in the forward peak. This feature shows that our model is not completely realistic, because it is known that at high energy the imaginary part of the scattering amplitude is greater than the real part. However, we do find the imaginary part becoming relatively more important as the energy is increased. Figure 1 shows the real and imaginary parts of the zero-angle elastic-scattering amplitude, for the case of all attractive potentials, as a function of p_1 , the incident center-of-mass momentum.

The real part of the forward elastic amplitude is very sensitive to errors in the elastic scattering phase shifts at high l . To get an accurate measure of $\text{Re}f_{11}(0)$, especially at high energy, we must go to a much smaller step size in the numerical integration, than is necessary for the rest of our results. For this reason we have only two good calculations of $\text{Re}f_{11}(0)$ —at 1.6 and 3.15 BeV/c lab momentum.

In addition to looking at the cross sections it is instructive to examine the behavior of the S -matrix

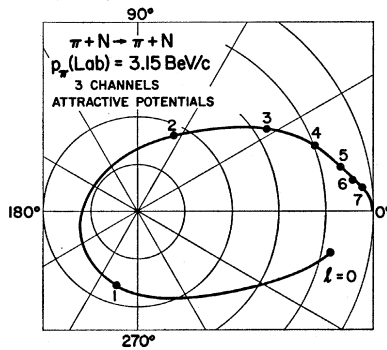


FIG. 2. The behavior of the calculated S -matrix element as a function of orbital angular momentum l for pion-nucleon elastic scattering at an incident pion laboratory momentum of 3.15 BeV/c. The calculations were done only at integral values of l , and the curve is merely drawn to aid the eye.

elements as a function of l . Of course we compute the S -matrix elements only for integer values of l . However we can draw smooth curves between the S -matrix elements for different values of l to aid the eye. Presumably, if we solved the radial Schrödinger equation for these intermediate values of l , the S -matrix elements would follow a path not too different from the one we draw. Besides graphs of η versus l , and δ versus l , we have drawn curves directly showing the motion of S in the complex plane, as l is varied. It has proved necessary to make these plots in order to try to get information about the absolute phase of the S matrix. The coupled-channel calculation gives the phases δ_i of the S matrix only modulo π (i.e., 180°). This fact does not lead to any ambiguity in the cross sections, since the expression for the cross sections contains the phases only in the factors $e^{2i\delta_i}$. However, in the approximation given by the Sopkovich formula, the square root of the S matrix enters. Thus, if a phase is altered by π , a real change occurs in the cross section predicted by Sopkovich's formula.

In a one-channel problem, the complex number S_l (the 1-by-1 S matrix) will move along on the unit

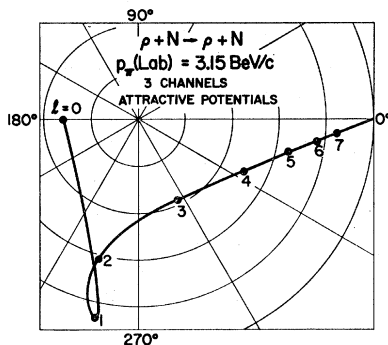


FIG. 3. The calculated S -matrix elements for ρ -nucleon elastic scattering versus l at the same energy in the c.m. system as in Fig. 2.

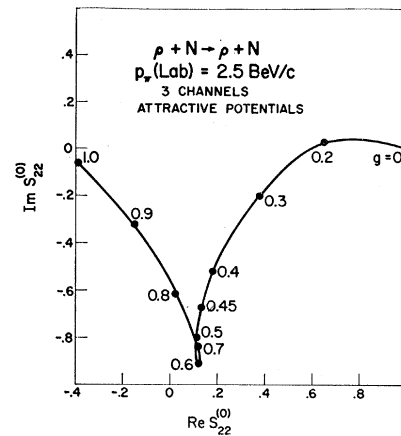


FIG. 4. The calculated s -wave S -matrix element for ρ -nucleon elastic scattering ($S_{22}^{(0)}$) as a function of the coupling strength g of the Yukawa potentials.

circle as the parameters of the problem, such as energy, coupling strength, or angular momentum l , are varied. Scattering is strongest when $S_l = -1$, and a resonance corresponds to S_l moving rapidly, counterclockwise, through the value -1 as the energy is increased. The behavior of the individual S -matrix elements $S_{\alpha\beta}^{(l)}$ in a coupled-channel problem is only qualitatively similar. Figures 2 and 3 show the traces in the complex plane made by some representative S -matrix elements at a given energy (incident pion momentum 3.15 BeV/c) as the parameter l is varied. We also found some very similar curves by plotting $S_{\alpha\beta}^{(0)}$ as a function of g , the over-all strength of our potential matrix. One of these is shown in Fig. 4. Here we are not handicapped by a discrete independent variable, and can obtain the curve in as much detail as necessary.

With a stretch of the imagination, all these curves might be regarded as distorted circles, the motion being counterclockwise (increasing phase shifts) as the strength of the coupling is increased, or, equivalently, as l is reduced. Figures 3 and 4 show the S -matrix elements for ρ -nucleon scattering rather than for

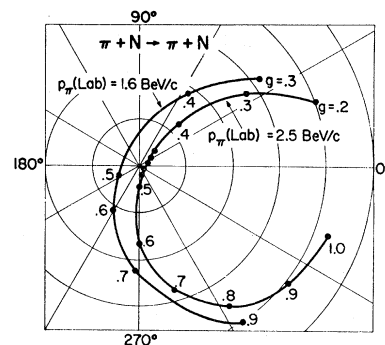


FIG. 5. Path of $S_{11}^{(0)}$ (the s -wave S -matrix element for pion-nucleon elastic scattering) as the coupling constant g is varied from 0.2 to 1.0.

π -nucleon scattering because the ρ -nucleon curves are more distorted from circles. To get a feeling for this behavior of S , we looked at a case in which the Schrödinger matrix equation can be diagonalized. If the Schrödinger equation is diagonalizable, the solution to an n -channel problem can be written in terms of the solution to a single channel problem, in which the paths of S -matrix elements are circles.

The Schrödinger equation can be diagonalized if the kinematics are the same in all channels and the elements of the potential matrix all have the same range. A detailed discussion of this problem in a four-channel case is given in the Appendix. A three-channel case can be done analogously. The S matrix turns out to be

$$S = I + \frac{1}{3}(e^{2i\delta} - 1) \begin{pmatrix} 1 & 1 & 1 \\ 1 & 1 & 1 \\ 1 & 1 & 1 \end{pmatrix}, \quad (19)$$

where δ and $e^{2i\delta}$ are the phase shift and S -matrix, respectively, for a one channel case. Here δ is just the eigenphase shift for this simple diagonalizable case. From Eq. (19) we see that the elastic S -matrix elements are all alike,

$$S_{\alpha\alpha} = \frac{2}{3} + \frac{1}{3}e^{2i\delta}, \quad (20)$$

and the inelastic elements are

$$S_{\alpha\beta} = -\frac{1}{3} + \frac{1}{3}e^{2i\delta}. \quad (21)$$

Equations (20) and (21) represent circles in the complex plane of radius $\frac{1}{3}$. If δ is monotonically increasing, $S_{\alpha\alpha}$ and $S_{\alpha\beta}$ will circulate counterclockwise. Resonant effects will show up here if $S_{\alpha\alpha}$ moves rapidly downward across the real axis at $\frac{1}{3}$. The extent to which it is a mistake to neglect the differences in ranges and masses, is shown by the extent to which

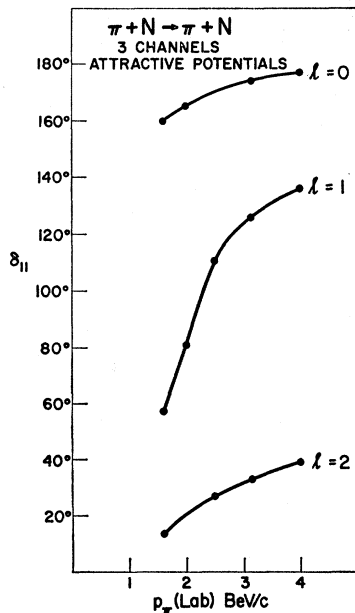


FIG. 6. Calculated pion-nucleon elastic scattering phase shifts $\delta_{11}^{(0)}$ as a function of laboratory pion momentum.

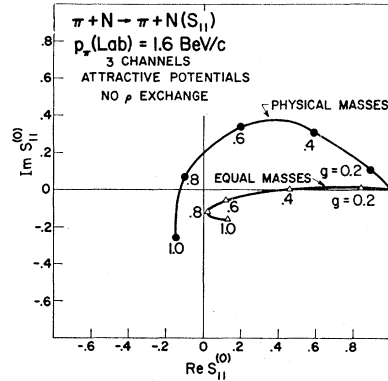


FIG. 7. The behavior of $S_{11}^{(0)}$ (calculated elastic pion-nucleon s -wave S -matrix element) as a function of the coupling strength. To show the effects of kinematics, we compare the case in which all particles have their actual masses (marked physical masses) with the case in which the incident particle has the pion mass and the target particle the nucleon mass in all three channels (marked equal masses).

these simple circular curves are distorted in the actual coupled channel results.

In Fig. 5 is illustrated the dilemma mentioned above about the choice of phase for use in Sopkovich's formula. At low energy the path followed by $S_{11}^{(0)}$, as the strength g is increased, encircles the origin, while at high energy, it does not. Since the square root in Sopkovich's formula introduces a branch point at the origin, it would seem that some procedure such as this is necessary to discover which branch to take. This criterion requires $\delta_{11}^{(0)}$ to be positive at low energy and negative at high energy. However, this seems very artificial since the behavior of $S_{11}^{(0)}$ as a function of the energy is very smooth (Fig. 6) and no special significance seems to attach to the question of whether or not the curve has encircled the origin. For this reason we have kept both cases, and in the cross section graphs, the curves labeled SF result from the assumption $\delta_{11}^{(0)} > 0$, and those labeled SF₋ from the assumption $\delta_{11}^{(0)} < 0$.

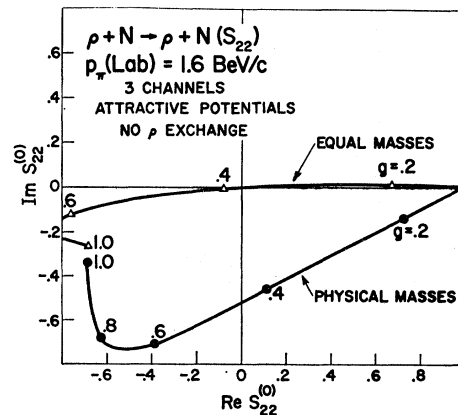


FIG. 8. The behavior of $S_{22}^{(0)}$ (calculated elastic ρ -nucleon s -wave matrix element as a function of the coupling strength). See caption to Fig. 7.

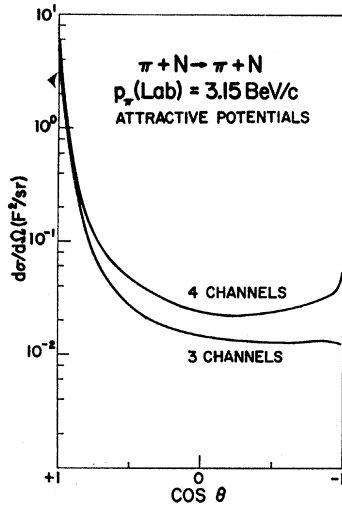


FIG. 9. A comparison of the calculated pion-nucleon differential cross section for elastic scattering in a three-channel case with the cross section in a four-channel case. The angle θ is the center-of-mass scattering angle of the meson in all figures.

For all the other channels and l values, we felt that the choice was relatively unambiguous.

One remarkable feature of the results obtained by solving the coupled channel equations is that $S_{22}^{(l)}$ always moves very quickly into the lower half-plane; in other words, except for very high l or very weak attractive potentials, $\delta_{22}^{(l)}$ is negative. This is true for all the cases we calculated, both 3- and 4-channel, regardless of the energy, or whether the diagonal potential was positive, negative, or zero. Therefore it would seem to be a kinematical effect. To check this idea, we went to the case of no ρ exchange, where all elements of the potential matrix are zero except for those off-diagonal elements where pion exchange is allowed. Using this potential, we did two calculations of the $l=0$ S matrix as a function of g : first with the same kinematics in all three channels, so that the

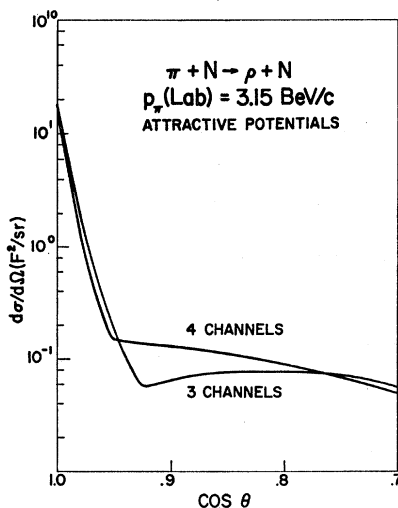


FIG. 10. A comparison of the calculated cross section for $\pi + N \rightarrow \rho + N$ in 3- and 4-channel cases.

problem is diagonalizable; second, with the actual particle masses, a case which is not diagonalizable. The results are shown in Figs. 7 and 8. In the first case, solution by diagonalization shows that $S_{22}^{(0)}$ should be just equal to $2S_{11}^{(0)} - 1$, and this behavior is demonstrated by our numerical results. In the second case, just changing the kinematics, we see a return of the familiar situation in which δ_{11} is strongly positive, and δ_{22} strongly negative.

This persistent sizable difference between S_{11} and S_{22} is noteworthy for the following reason. In applying Sopkovich's formula to an actual experiment, such as ρ production, one needs to know S_{22} , the S -matrix element for elastic ρ -nucleon scattering, which of course is totally unknown. Thus the procedure usually adopted is to assume $S_{22} = S_{11}$. In our model, this is a bad approximation, despite the fact that we have used identical interactions for the π and ρ mesons; the mass difference between the π and ρ alone is responsible. Further demonstration of the difference between these two elastic elements is given in Fig. 22 of the next section.

In the upper portion of our energy range, it is energetically feasible to produce the ρ and the Δ resonances together. Therefore, at incident lab momentum 3.15 BeV/c, we performed a 4-channel calculation in which the ρ - Δ channel was added to the other three (πN , ρN , $\pi \Delta$), still ignoring spins, of course. All the coupling constants $g_{\alpha\beta}$ were set equal to one, as they were in the 3-channel calculation at the same energy. However, we get in this way an effectively stronger interaction, in the sense that the total cross section is increased by the addition of another channel, especially since this new channel is coupled to the incident channel by the strong π -exchange potential. The results are qualitatively the same for the 3- and 4-channel cases. The increase in the elastic scattering cross section is shown in Fig. 9; a decrease in the ρ -production forward peak, presumably due to increased competition from the fourth channel, can be seen in Fig. 10. A typical comparison of results for the behavior of an S -matrix element as a function of l , is shown in Fig. 11; here the elastic element S_{11} is seen to curl around further in the

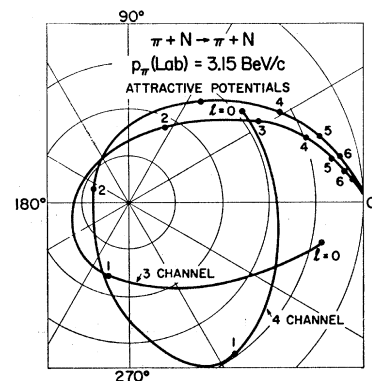


FIG. 11. A polar plot of S_{11} as a function of l in the 3- and 4-channel cases.

4-channel case, reflecting the effectively stronger interaction.

IV. COMPARISON OF THE APPROXIMATION METHODS WITH A COUPLED-CHANNEL CALCULATION

We here consider the question of the circumstances under which the various approximation methods give a significant improvement over the Born approximation. We also consider the related question of under what circumstances the approximation methods closely reproduce the exact solution of our model. In asking these questions we may take two points of view: On the one hand, if we regard the approximation methods as being simple phenomenological models with no theoretical justification, then we are simply interested in how well the models reproduce the coupled-channel cross sections. On the other hand, if we wish to examine the validity of the approximations in more detail, then we ask to what extent do the approximation methods reproduce the S -matrix elements given by the coupled-channel calculation.

We have found that under certain circumstances the cross sections are given rather well by the approximation method, at least near the forward direction, but that the S -matrix elements are quite different from the S -matrix elements of the coupled-channel calculation in the low partial waves. This correlation is understandable. If the S -matrix elements are rather good in

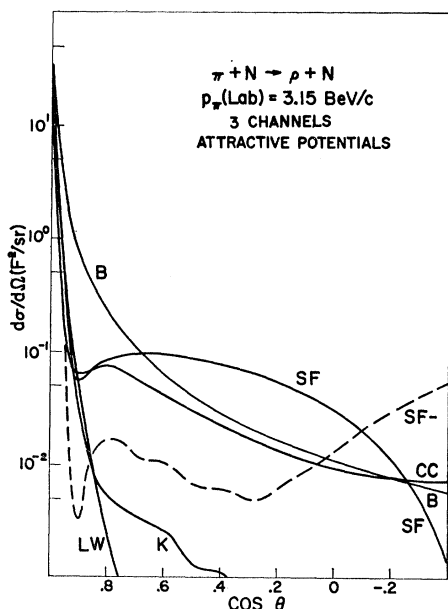


FIG. 12. A comparison of the differential cross sections for the reaction $\pi+N \rightarrow \rho+N$ calculated by different methods. The curve marked CC is the exact coupled-channel solution to the model. The curve marked B is the Born approximation, K stands for the K -matrix approximation, SF for Sopotovich's formula, and LW for the method of Lichtenberg and Williams. All these methods are described in more detail in the text.

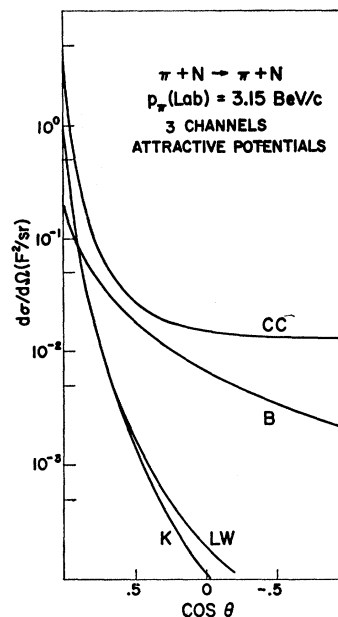


FIG. 13. A comparison of the pion-nucleon differential cross section for elastic scattering as calculated by various methods. For explanation of the letters on the curves, see the caption to Fig. 12. There is no curve marked SF, since curve marked CC is input information in Sopotovich's method.

the high partial waves, which correspond to peripheral interactions, then the cross sections should be rather good near the forward direction. The low partial waves contribute to the cross sections at large angles, and if these partial waves are not treated properly, the large-angle results will not be accurate.

We shall now compare the various methods in somewhat more detail, beginning with the three-channel problem at 3.15 BeV/c.

First we look at the inelastic scattering $\pi+N \rightarrow \rho+N$ on a semilogarithmic plot, Fig. 12. This is the channel where the approximation method should be the best. The Born approximation is too large, and therefore

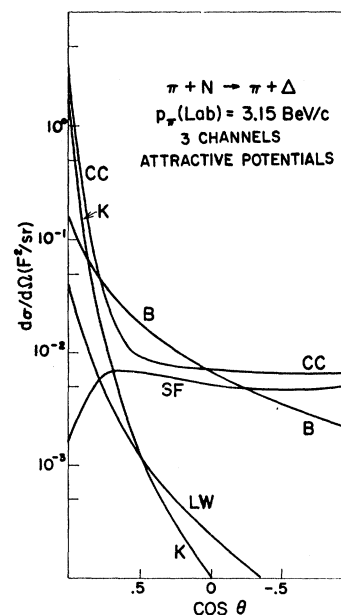


FIG. 14. A comparison of the various calculated differential cross sections for the reaction $\pi+N \rightarrow \pi+\Delta$, where Δ is the pion-nucleon resonance at 1238 MeV. For explanation of the letters, see the caption to Fig. 12.

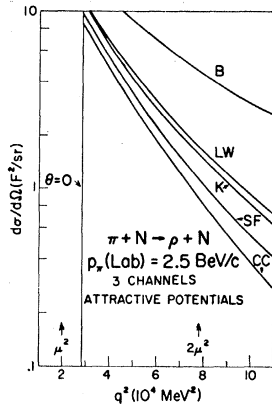


FIG. 15. A comparison of the various calculated cross sections for $\pi+N \rightarrow \rho+N$ versus squared 3-momentum transfer q^2 at an incident momentum of 2.5 BeV/c. Here μ is the pion mass.

using absorption parameters ought to improve the agreement with the experiment. We see that between $\cos\theta=1$ and $\cos\theta=0.9$, corresponding to a region of three-momentum transfer given by $140 < q < 500$ MeV/c, the agreement between the approximate solutions and the coupled-channel results is rather good.

However, we see that at large angles, $\cos\theta < 0.8$, the Born approximation actually gives better agreement with the coupled-channel result than any of the approximation methods. However, this should not be taken seriously, since the cross section has fallen two orders of magnitude or more and the peripheral model is not valid for $\cos\theta < 0.8$, which is to say for $q > 5\mu$, where μ is the pion mass. The two curves marked SF and SF₋ need some explanation. The curve marked SF₋ is that curve which is obtained by changing the s -wave phase shift $\delta_{11}^{(0)}$ of the coupled-channel calculation by π , making it a small negative rather than a large positive phase. If we had changed all the phase shifts by π we would get no change in the cross section, but changing the s -wave phase by π relative to all the other phases and then taking the square root in Sopotovich's formula leads to the differences shown in the figure. However, in the forward angles the differences between these two cases are not nearly so large. The higher the energy, the less important this s -wave phase shift becomes.

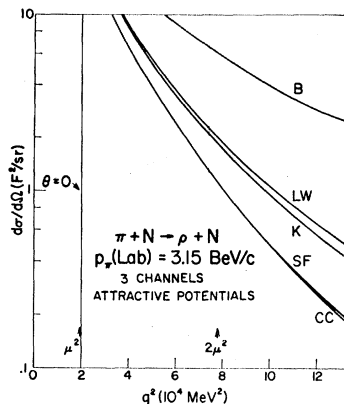


FIG. 16. Same as Fig. 15 at 3.15 BeV/c.

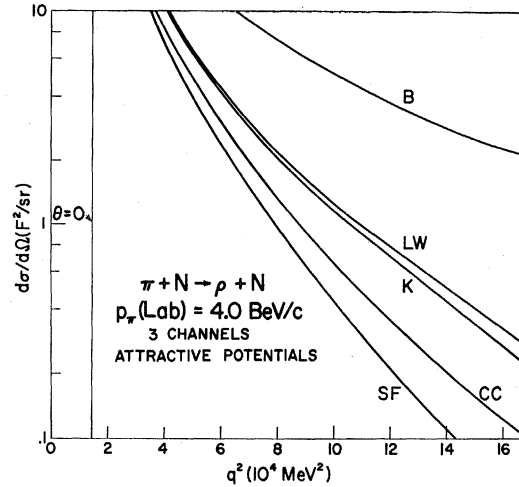


FIG. 17. Same as Fig. 15 at 4.0 BeV/c.

Figure 13 shows the elastic scattering cross section $\pi+N \rightarrow \pi+N$ on a semilogarithmic scale over the whole angular region. We see from the figure that at large angles the Born approximation result is closer to the coupled channel calculation than either of the two other approximation methods, which are supposedly improvements on the Born approximation. However, near the forward direction, where the cross section is appreciable, the modified approximation methods are better. At the large angles the cross section has dropped more than two orders of magnitude and is negligible. There is no curve marked SF for elastic scattering, since the coupled-channel results (CC) are input data in Sopotovich's method.

We next show the inelastic channel $\pi+N \rightarrow \pi+\Delta$ (Fig. 14). This is a ρ -exchange channel, and the Born approximation result is quite a bit smaller than the

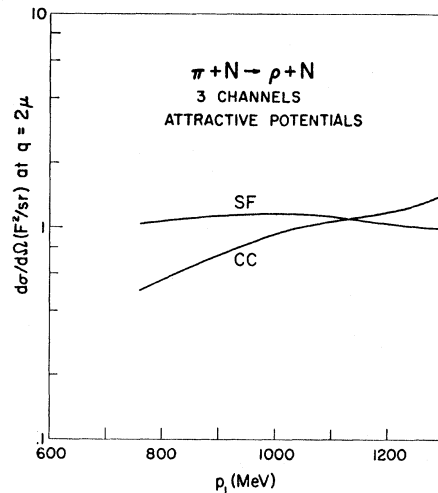


FIG. 18. Calculated cross sections for $\pi+N \rightarrow \rho+N$ at fixed 3-momentum transfer ($q=2\mu$) as a function of the incident CM momentum p_1 .

FIG. 19. A comparison of calculated cross sections for $\pi+N \rightarrow \rho+N$ at incident momentum 1.6 BeV/c with attractive potentials.

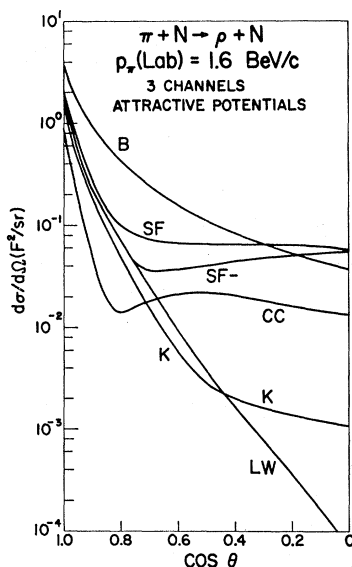
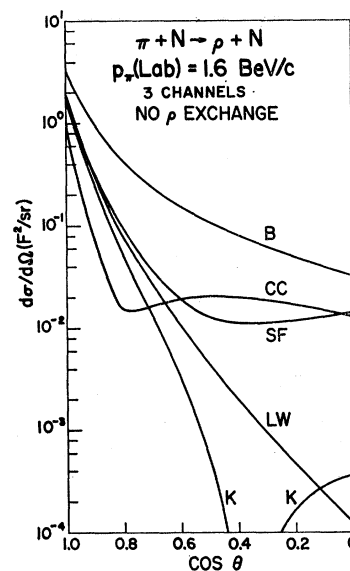


FIG. 21. Same as Fig. 19 with only π -exchange potentials (ρ -exchange potentials are set equal to zero).



coupled channel result. When this is the case, use of Sopkovich's formula, which reduces the Born approximation still further, cannot be expected to lead to improvement with experiment at any angle. The K -matrix method, however, employing exact unitarity, does give considerable improvement for small angles. The results presented in Figs. 12, 13, and 14 for lab momenta of 3.15 BeV/c, are very similar to those obtained at our other momenta (1.6, 2.0, 2.5, 4.0) using the same potentials.

Because we are dealing with a peripheral model, we are principally interested in small-angle scattering, with momentum transfers q of a few pion masses; moreover, the approximations we are studying are of use mainly on the forward peak in the differential cross section for ρ production. Using an expanded scale

to show this peak in detail, we find an amazingly good agreement between Spokovich's formula and exact results at 3.15 BeV/c. However, the agreement does not persist at other energies: the SF curve is too high at 2.5 and too low at 4.0. The other approximations give cross sections which are too high for small momentum transfers at all energies considered. Figures 15, 16 and 17 show the small-angle ρ production cross section as a function of squared 3-momentum transfer q^2 , for lab momenta of 2.5, 3.15, and 4.0 BeV/c, respectively. All the approximation methods are significantly better than Born approximation in these cases, with Sopkovich's formula seemingly the best. The energy dependence of the SF and exact cross sections is shown in Fig. 18, where the cross sections at fixed momentum

FIG. 20. Same as Fig. 19 with repulsive potentials.

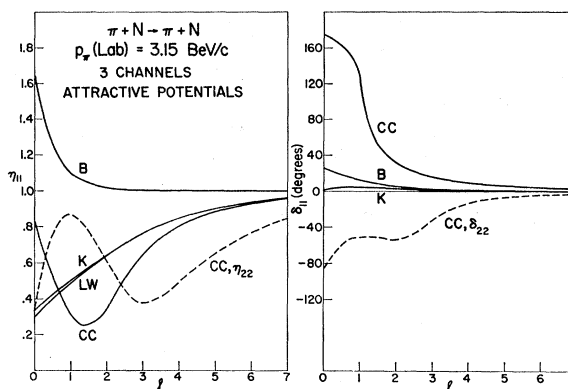
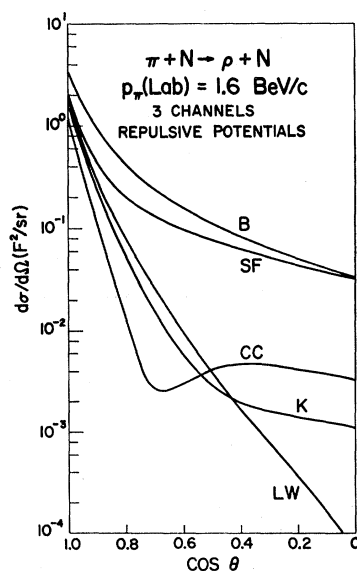


FIG. 22. A comparison of the absorption parameters η_{11} and real phases δ_{11} for pion-nucleon elastic scattering as a function of l , as calculated by various methods. The values of δ and η are computed only for integral values of l , and the curves are drawn merely to aid the eye. There is no curve marked SF, since the Sopkovich method allows one to calculate η for inelastic processes. The δ 's are all 0 in the LW approximation. Also shown are the coupled-channel results for η_{22} and δ_{22} (ρ -nucleon elastic scattering), since certain approximation methods assume that $\eta_{22} = \eta_{11}$ and $\delta_{22} = \delta_{11}$.

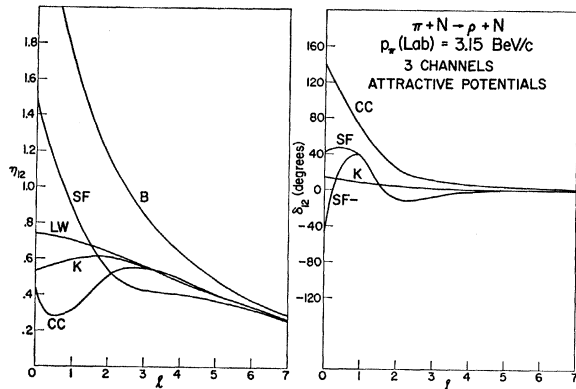


FIG. 23. A comparison of the absorption parameters η_{12} and real phases δ_{12} for the reaction $\pi+N \rightarrow \rho+N$ as a function of l , as calculated by various methods.

transfer $q=2\mu$ are plotted against p_1 , the initial-state center-of-mass momentum. We might mention that 3.15 BeV/c was the first momentum at which we did any calculations, and that it was chosen for the largely irrelevant reason that some experimental data existed at that energy. Yet we chose the one energy at which Sopkovich's formula method gives essentially perfect agreement with the exact solution of our Schrödinger equation model for the cross section at forward angles.

Next let us look at the cross sections for different signs of the potentials. So far we have been discussing the case of all attractive potentials at different energies. Because we found only smooth and rather weak energy dependence, we did the following calculations all at 1.6 BeV/c where the longer wavelength makes the integration of the differential equations easier. Also we consider the effect of neglecting the ρ -exchange potentials entirely.

If the coupling constants $g_{\alpha\beta}$ of all the π -exchange potential elements are kept equal to a single constant, g_π , then the cross sections in all channels are independent of the sign g_π . The reason for this is that the π -exchange potential always changes a π -meson state into a ρ -meson state, or vice versa: thus any given scattering amplitude is a sum of terms which are either all odd or all even in g_π . So the case of attractive π -exchange and repulsive ρ -exchange is identical to that of all repulsive potentials, and the case in which those two signs are reversed is the same as the all-attractive case.

Figures 19, 20, and 21 show the differential cross section for ρ production at 1.6 BeV/c in the following three cases, respectively: all attractive potentials; all repulsive potentials; attractive π exchange and zero ρ exchange. The Born approximation is exactly the same for all three of these cases; the K and LW (Lichtenberg-Williams) methods give the same results for the first two cases. Qualitatively the three cases are quite similar in that all three approximation methods are too large in the forward peak, although about the right shape.

We leave to the reader to decide whether these approximate results are "good enough." None of the approximation methods seems to be trustworthy at larger angles, although Sopkovich's method does fairly well in the case with no ρ exchange.

Up to now we have been comparing cross sections, but the approximation methods we are testing involve formulas for the S -matrix elements. Therefore we can study the approximations in somewhat more detail by a direct comparison of the approximate and exact S matrices. We shall show plots of the absorption parameters η and the real phases δ_l as a function of l . Again the curves are merely to aid the eye, as the Schrödinger equation is solved only for integral values of l .

Figure 22 shows S_{11} , the elastic S -matrix element for πN scattering, at 3.15 BeV/c. (Actually shown are η_{11} and δ_{11} , where $S_{11}=\eta_{11}e^{2i\delta_{11}}$.) Also drawn in the same figure for comparison is the exact result for S_{22} , the element giving ρN elastic scattering. The difference between S_{11} and S_{22} , which was stressed in Sec. III, is clearly seen here, too.

The reaction $\pi+N \rightarrow \rho+N$, in which we are most interested, is produced by S_{12} , which is shown in Fig. 23. All three of the methods do fairly well in predicting η_l , after the first few partial waves. It seems to be a general feature, however, that the agreement is poorer with regard to δ_l . We can see no reason, from studying these graphs, for the excellent agreement between the SF and exact cross sections in the forward peak at this energy (see Fig. 16). In fact, methods LW and K seem to be better than SF, if anything, in their predictions for η_l , and none of the methods give particularly good agreement with δ_l . The high partial waves are important for the forward peak, but for $l>7$, not shown on the graph, methods LW and K are fully as good as SF. On the other hand, when the negative S -wave phase is put into Sopkovich's formula (SF₋), the agreement in the cross sections is spoiled, so the larger δ_l given by the SF method for $l=0, 1$ may be a factor of some importance. At any rate, it is clear that the good agreement in the forward cross sections at 3.15 BeV/c, does not reflect any detailed agreement between Sopkovich's formula and exact S -matrix elements. The fact that all the methods give about the right shape in the forward peak, however, is a reflection of the fact that for l greater than about 4, the approximation schemes all give a good prediction of η_l , which is the important quantity for inelastic scattering at high l .

V. CONCLUSIONS

We have seen in our model that when the Born approximation for nondiagonal processes is too large, use of approximation methods to unitarize the S -matrix elements, partially or completely, does bring improvement in the agreement with the coupled-channel calculation at small angles where the peripheral model

is expected to hold best. At large angles there are large differences among the various methods, but one should not expect any peripheral model, even the coupled-channel model, to describe events accurately here. The straightforward use of Sopkovich's formula, where the elastic-scattering parameters are taken from experiment, of course yields no prediction for the elastic scattering. The other methods do not seem to yield much improvement over the Born approximation when compared with coupled-channel results for the elastic scattering, at least not in a three-channel problem. For a channel in which the Born approximation is too small, only a method like the K -matrix method takes into account unitarity sufficiently accurately can improve upon the Born approximation result. But of course no one would apply Sopkovich's formula to a nondiagonal channel in which the Born approximation is already too small.

In the usual application of Sopkovich's method to analysis of experimental data it is assumed that the S -matrix element $S_{\alpha\beta} = i(S_{\alpha\alpha})^{1/2}B_{\alpha\beta}(S_{\beta\beta})^{1/2}$ can be calculated with reasonable accuracy by assuming that $S_{\alpha\alpha} = S_{\beta\beta}$. In the coupled-channel calculation done here we have found that this is not a good approximation. Further, since the difference between $S_{\alpha\alpha}$ and $S_{\beta\beta}$ arose solely from differences in the kinematics in the two channels it is hard to see how this assumption can be justified, except possibly at energies much higher than those considered here. It was also found that the real part of the phase shift is not negligible, a fact which means that $S_{\alpha\alpha}$ cannot be treated as a real number. Since a square root of $S_{\alpha\alpha}$ is involved it is necessary to ascertain the correct phase. Both the correct phase and the elastic scattering in the channel β (in our calculation channel β would be $\rho N \rightarrow \rho N$) are not usually obtainable from the available experimental data.

The method of Lichtenberg and Williams neglects the real part of the phase shift, a procedure which is not justified by the coupled channel calculations. It is interesting however that it does predict the absorption parameter η_l correctly, i.e., in agreement with the coupled channel η_l , after the first few l values.

It may be possible that the approximation methods discussed in this paper are more justified when applied to the Feynman diagrams of field theory than when applied to a potential model. However, the burden of proof would appear to lie with those who wish to claim that this possibility holds.

ACKNOWLEDGMENTS

The authors should like to thank Professor R. G. Newton and Professor E. J. Konopinski for interesting discussions.

APPENDIX: DIAGONALIZATION PROCEDURE

If all the channels have the same kinematics and if all elements of the potential matrix have the same range,

then the coupled channel Schrödinger equations can be uncoupled by diagonalization. Written in matrix form, the equations are:

$$I\Psi''(r) + \{P^2 - [l(l+1)/r^2]I\}\Psi(r) - 2\Lambda V\Psi(r) = 0. \quad (A1)$$

Here Ψ , P^2 , Λ , and V are matrices with elements as follows:

$$\begin{aligned} \Psi_{\alpha\beta} &= \mu_{\beta\alpha}^{(l)}(r), & P_{\alpha\beta}^2 &= \delta_{\alpha\beta}p^2, \\ \Lambda_{\alpha\beta} &= \delta_{\alpha\beta}\lambda_\alpha, & V_{\alpha\beta} &= V_{\alpha\beta}(r). \end{aligned} \quad (A2)$$

Under the assumption of equal kinematics, $P^2 = p^2I$, and $\Lambda = \lambda I$:

$$\left[\left(\frac{d^2}{dr^2} + p^2 - \frac{l(l+1)}{r^2} \right) I - 2\lambda V \right] \Psi = 0. \quad (A3)$$

Under the assumption of equal ranges $V = -gUe^{-\mu r}/r$, where U is some symmetric r -independent matrix. Now choose a unitary constant matrix A to diagonalize U : $A^\dagger UA = U'$, where U' is diagonal. If Eq. (3) is multiplied by A^\dagger from the left and by A from the right, the result is a diagonal matrix equation, that is, a set of uncoupled Schrödinger equations:

$$\begin{aligned} A^\dagger \left\{ \left[\frac{d^2}{dr^2} + p^2 - \frac{l(l+1)}{r^2} \right] I + 2\lambda g \left(\frac{e^{-\mu r}}{r} \right) U \right\} A A^\dagger \Psi A &= 0 \\ \left\{ \left[\frac{d^2}{dr^2} + p^2 - \frac{l(l+1)}{r^2} \right] I + 2\lambda g \left(\frac{e^{-\mu r}}{r} \right) U' \right\} \Psi'(r) &= 0, \end{aligned} \quad (A4)$$

where $\Psi' = A^\dagger \Psi A$.

Let S' be the diagonal S matrix resulting from the solution of Eq. (4). This means that for large r ,

$$\Psi' \sim [(2l+1)/2] r i^l [S' h_l^{(1)}(pr) + I h_l^{(2)}(pr)]. \quad (A5)$$

On the other hand, if S is the S matrix resulting from the original problem [Eq. (3) with $V = -gUe^{-\mu r}/r$], then for large r ,

$$\Psi \sim [(2l+1)/2] r i^l [S h_l^{(1)}(pr) + I h_l^{(2)}(pr)]. \quad (A6)$$

But we know that $\Psi = A\Psi'A^\dagger$, so S can be obtained easily from S' :

$$\Psi \sim [(2l+1)/2] r i^l [A S' A^\dagger h_l^{(1)}(pr) + I h_l^{(2)}(pr)]. \quad (A7)$$

Therefore

$$S = A S' A^\dagger. \quad (A8)$$

For example, in the 4-channel case with all ranges and kinematics, as well as coupling constants, assumed equal, we have

$$U = \begin{pmatrix} 1 & 1 & 1 & 1 \\ 1 & 1 & 1 & 1 \\ 1 & 1 & 1 & 1 \\ 1 & 1 & 1 & 1 \end{pmatrix}.$$

This is diagonalized by

$$A = \frac{1}{2} \begin{pmatrix} 1 & -1 & -1 & -1 \\ 1 & -1 & 1 & 1 \\ 1 & 1 & -1 & 1 \\ 1 & 1 & 1 & -1 \end{pmatrix},$$

giving

$$U' = \begin{pmatrix} 4 & 0 & 0 & 0 \\ 0 & 0 & 0 & 0 \\ 0 & 0 & 0 & 0 \\ 0 & 0 & 0 & 0 \end{pmatrix}, \quad S' = \begin{pmatrix} e^{2i\delta} & 0 & 0 & 0 \\ 0 & 1 & 0 & 0 \\ 0 & 0 & 1 & 0 \\ 0 & 0 & 0 & 1 \end{pmatrix} = I + iT',$$

$$T' = t \begin{pmatrix} 1 & 0 & 0 & 0 \\ 0 & 0 & 0 & 0 \\ 0 & 0 & 0 & 0 \\ 0 & 0 & 0 & 0 \end{pmatrix}, \quad T = AT'A^+ = \frac{1}{2}t \begin{pmatrix} 1 & 1 & 1 & 1 \\ 1 & 1 & 1 & 1 \\ 1 & 1 & 1 & 1 \\ 1 & 1 & 1 & 1 \end{pmatrix}$$

$$S = 1 + iT.$$

Thus, in this case there is only one single-channel Schrödinger equation to solve for each l value. We did this case both with the coupled-channel program and by integrating the one-channel equation and then carrying out the matrix transformation (numerically, of course). The two methods were in satisfactory numerical agreement.

Theory of Parity-Violating Nonleptonic Decay*

S. P. ROSEN

Purdue University, Lafayette, Indiana

(Received 8 November 1965)

The simplest way of explaining the result $A(\Sigma^+ | n\pi^+) = 0$ is to assume an effective parity-violating Hamiltonian of the form $(\bar{B} \times B)_{(8)} \times \pi$. With no further assumptions, this Hamiltonian predicts two sum rules which are closely related to the Lee-Sugawara triangle, and it imposes an isotopic-spin selection rule $\Delta T < \frac{1}{2}$. The proposed coupling scheme is a consequence of several dynamical models, and the $\Delta T < \frac{1}{2}$ rule is consistent with the data on $K \rightarrow 2\pi$.

1. INTRODUCTION AND GENERAL THEORY

A RECENT experiment¹ indicates that the parity-violating (pv) amplitude for $\Sigma^+ \rightarrow n\pi^+$ is zero. Starting from this result, we discuss a general theory which predicts two sum rules for the pv amplitudes of nonleptonic hyperon decay. These sum rules are related to the Lee-Sugawara triangle,² but they do *not* depend for their validity upon such assumptions as octet transformation properties and the $\Delta T = \frac{1}{2}$ rule; instead they follow from one simple assumption about the coupling of baryons and antibaryons in the effective Hamiltonian. We make a comparison with experimental data and discuss models which give rise to the desired coupling.

In unitary symmetry space,³ the most general form of the effective Hamiltonian for nonleptonic hyperon decay is

$$\sum_{m,n} C_{mn} [(\bar{B} \times B)_{(m)} \times \pi]_{(n)} \quad (m, n = 1, 8, 10, \bar{10}, 27), \quad (1)$$

where B and \bar{B} denote the baryon and antibaryon octets, respectively, and (m) denotes the $SU(3)$ representation to which they are coupled. The symbol π represents the pseudoscalar meson octet and (n) denotes the over-all $SU(3)$ transformation properties of each term in Eq. (1). The coefficients C_{mn} are arbitrary coupling constants.

The decay mode $\Sigma^+ \rightarrow n\pi^+$ arises from a term $(\bar{\Sigma})^- n\pi^+$ in Eq. (1). [Note that $(\bar{\Sigma})^-$ corresponds to the antiparticle of Σ^+ .] Because the combination $(\bar{\Sigma})^- n$ has isotopic spin $T = \frac{3}{2}$, it cannot appear in an octet $(\bar{B} \times B)$ system.⁴ Therefore the simplest way of ensuring that¹

$$A(\Sigma^+ | n\pi^+) = 0 \quad (2)$$

is to take an effective pv Hamiltonian of the form

$$H_{pv} = \sum_n d_n [(\bar{B} \times B)_{(8)} \times \pi]_{(n)} \quad (n = 8, 10, \bar{10}, 27). \quad (3)$$

Because of the occurrence of the (10), ($\bar{10}$), and (27) representations in Eq. (3), H_{pv} can include an admixture of $\Delta T = \frac{1}{2}$ and $\frac{3}{2}$, but not $\Delta T = \frac{5}{2}$. In tensor notation,⁵ the relevant types of terms are

$$\Delta T = \frac{1}{2}: \quad L_2^3, \bar{M}_{12}^{13}, (N_{12}^{13} + N_{22}^{23}), \quad (4a)$$

$$\Delta T = \frac{3}{2}: \quad M_{22}^{23}, (2N_{12}^{13} - N_{22}^{23}), \quad (4b)$$

and their Hermitian conjugates. L , M , \bar{M} , and N

* Supported in part by the U. S. Air Force.

¹ M. Bazin, H. Blumenfeld, U. Nauenberg, L. Seidlitz, R. J. Plano, S. Marateck, and P. Schmidt, Phys. Rev. **140**, B1358 (1965).

² B. W. Lee, Phys. Rev. Letters **12**, 83 (1964); H. Sugawara, Progr. Theoret. Phys. (Kyoto) **31**, 213 (1964).

³ M. Gell-Mann, California Institute of Technology Report No. CTSL-20, 1961 (unpublished); Y. Ne'eman, Nucl. Phys. **26**, 222 (1961).

⁴ S. P. Rosen and S. Pakvasa, Phys. Rev. Letters **13**, 773 (1964).

⁵ S. Okubo, Progr. Theoret. Phys. (Kyoto) **28**, 24 (1962).